Proceedings of the 7th International Conference on Civil Structural and Transportation Engineering (ICCSTE'22)
Niagara Falls, Canada – June 05-07, 2022
Paper No. 207
DOI: 10.11159/iccste22.207

Influence of Blend Ratio on Compressive Strength of Soda Ash Activated Fly Ash and Copper Slag Pastes

I.O. Erunkulu[1*], G. Malumbela[1], and O.P. Oladijo[2]
[1] Department of Civil and Environmental Engineering, Botswana International University of Science and Technology, Botswana
[2]Department of Chemical, Materials and Metallurgical Engineering, Botswana International University of Science and Technology, Botswana
* Corresponding Author, email address: ibukunerunkulu@gmail.com

Abstract
In this study, alkaline activated binder pastes were produced from high calcium fly ash and copper slag in different combinations. The blends were activated with soda ash (sodium carbonate) as the alkaline activator to effectively optimize each materials component in the development of the binder. The as-received samples and the hardened fly ash-copper slag paste were characterized using X-ray Diffraction, X-ray Fluorescence for chemical phase and elemental composition. The mechanical properties were determined by compressive strength test on the hardened cubes produced from resulting pastes at 3, 7, 28 days kept under varying curing conditions. The results show the effects of blend ratio, variation in individual material composition, and curing conditions at different activator dosages on compressive strength of the fly ash-Copper slag activated pastes. From the compressive strength tests result, the optimum composition for fly ash and copper slag was 60% and 40% respectively. Increase in soda ash dosage and curing temperature also increased material strength.

Keywords: Copper slag, High calcium fly ash, Alkaline activation, soda ash, paste characterisation

1. Introduction

The possible synthesis of binders possessing cementitious properties from the alkaline activation of aluminosilicate materials has been extensively explored in several studies [1]–[9]. Alkaline activated materials (AAM) are formed from the reaction of materials rich in aluminosilicate known as precursors with an alkaline solution at ambient or controlled temperatures. Widely used precursors are fly ash from coal-fired plants, metallurgical slags, and metakaolin [10] while sodium hydroxide and sodium silicate have been the activators of choice. The potential utilisation of aluminosilicates sources from industrial wastes makes AAM synthesis advantageous for environmental sustainability considerations asides from the low CO_2 emission attribute.

A frequent form of slag used in AAM is blast furnace slag (BFS), a by-product of steel mill obtained from the smelting of iron ore, limestone, and coke at higher temperatures. BFS is known to contain both anions of $(SiO_4)^{4-}$, $(AlO_4)^{5-}$ and $(MgO_4)^{6-}$ for network forming and Ca^{2+}, Al^{3+}, Mg^{2+} cations network modifying [11]. There are however other forms of slag with promising potential for activation whose chemical composition and physical properties vary in comparison to the former such as copper slag, nickel slag, phosphorus slag, steel slag, and other metallurgical slags.

Copper slag (CS) is derived from the smelting of copper ore. In contrast to BFS, CS is generally black containing majorly iron oxide, silica and lesser amounts of calcium oxide and alumina. Significant influence on the chemical composition variation in CS from different locations is the composition of the ore, process of smelting, and additives [12]. Typical range reviewed by the authors for CS are Fe_2O_3 (20.4-57.42%), SiO_2 (9.57-39.14%), Al_2O_3 (2.79-11.5%), CaO (1.96-26.1%), minor constituent of MgO (0.57-4.66%) and other oxides. These minute essential oxides compositions may explain the limited alkaline activation studies on the use of CS in developing AAM including the effect of high Fe_2O_3 content on the material activation. The presence of a substantial iron amount in the precursor is generally viewed to interfere with strength development in the activated product. [13] however, established the prevalence of other factors as the chemical and mineralogical form of the iron present to influence reactivity.

The potential of CS to release Al and Si based on activator type used was established by [14]. NaOH activators resulted in the fastest product structural build-up. [15] investigated the influence of parameters such as activator dosage, curing condition, and curing age on microstructural as well as strength development of alkali-activated copper-nickel slag. Optimum Na_2SiO_3 dosage was 8% for compressive strength of 17 MPa at 28 days. Higher dosages were found to decrease the material compressive strength. Similarly, [12]in their activation of CS with Na_2SiO_3 and NaOH activators, activator concentration lesser than 6% failed to develop products of significant strength above 2MPa after 28 days.

The replacement of basic pozzolanic material with other materials tends to change its binding characteristics[16]. modification of SiO_2/Al_2O_3 ratio in products by combining two different sources of aluminosilicate material and modifying the blend ratios can improve the compressive strength [17]. Although much attention has been given to the activation of fly ash/GGBFS blends using sodium hydroxides and silicates[18]–[20], the activation potential of copper slag and fly ash blends has not been extensively studied. Particularly the use of moderately alkaline activators such as soda ash in the activation. The use of sodium carbonate activator remains beneficial from a commercial stand view since they are less expensive and has ease of handling compared to commonly used activators [21].

This study aimed to investigate the influence of blend ratio and curing temperature in alkaline activated fly ash and copper slag with soda ash activation on compressive strength and chemical composition of the product. Pastes products were characterised by X-ray fluorescence (XRF) and X-ray diffraction (XRD) techniques in addition to compressive strength testing.

2. Materials and Experimental Program

2.1. Materials

Materials used in the paste synthesis for this study include fly ash, copper slag, and soda ash. Chemical composition of material is presented in table 1. The physical features of the fly ash and copper slag sample used is as seen in Fig. 1. High calcium fly ash samples from a local plant Morupule B (M_B) in Botswana was used in this study. The ash was collected at different times to give a typical representation. The as-received fly ash samples were quartered and coned before being mixed thoroughly for representative sampling of the ash used in the study. Thereafter, sieving of samples to remove extraneous material from the ash.

Slag samples were collected from the BCL slag dump at Selewe Phikwe. The as-received sample were milled to 32 microns and below to increase the surface area, and to obtain some degree of fineness for particles that can enhance the process of reaction [22]. The chemical composition of the milled slag is shown in Table 1. The iron oxide content of 59.10% in the sample is higher than the 20.4-57.42% range reported by [12] and a low-calcium slag of 2.72%. The slag sample was blended at 0%, 20%, 30%, 40%, and 50% by mass replacement of fly ashes used.

Table 1 Oxide composition of fly ash, copper slag and soda ash

Material	SiO_2	Al_2O_3	CaO	Fe_2O_3	SO_3	MnO	Na_2O	MgO	TiO_2	K_2O
Fly ash 1 (M_B)	33.28	26.16	20.54	6.82	8.52	0.21	0.61	1.17	1.95	0.32
Copper Slag	23.89	5.26	2.72	59.10	2.12	0.05	0.81	2.80	0.29	0.74
Soda ash	-	-	-	-	-	-	99.50	-	-	-

Sodium carbonate also known as soda ash was the only alkaline activator tested in this study. The grade used was soda ash dense from Botswana Ash (Pty) Ltd. Chemical properties of this grade as tested include 99.5% of Na_2O as shown in table 1 and average pH of 11.03 in solution at room temperature. The soda ash granules were used at 32% and 40% by weight of aluminosilicate source materials. Preparation for its use in the activation process required pulverisation with minimal atmospheric exposure while milling. Decisions on this procedure was from an earlier observation recorded in preceding experiments.

Figure 1: Sample feature of (a) Milled copper slag (b) MB fly ash

(a) (b)

2.2. Experimental Procedure

The experimental program undertaken in this study was designed considering four variables. Namely, precursor mix ratio (FA/C_S), curing temperature (25, 45, 65, 80 °C), activator concentration (0.32, 0.40) and curing days (3, 7, 28). However, the water content was maintained for all prepared mix. The effect of each variable is evaluated from observed properties after testing.

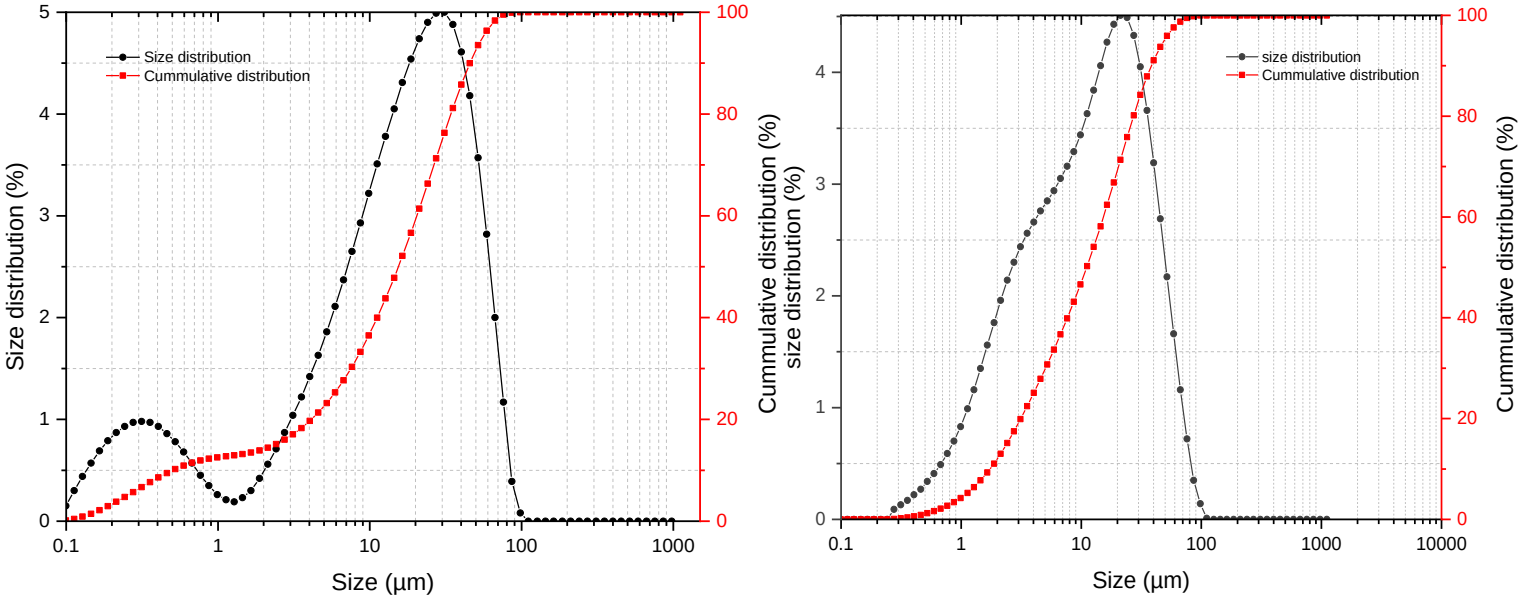

(a) (b)

Figure 2: Particles size distribution of (a) MB fly ash (b) copper slag

2.2.1. Source Material and Paste Characterisation

Characterisation techniques for the materials included particle size analysis, X-ray fluorescence (XRF) test as well as X-ray diffraction (XRD). Particle size analysis for both FA and slag was performed using the laser-based Malvern Mastersizer. The distribution of particle sizes is shown in Fig. 2. The physical properties investigated were average mean size of 21.24 µm and 17.26 µm for FA and copper slag respectively. MB ash exhibits multimodal distribution while CS particles have better size distribution range between 0.2 and 100 µm.

Determination of the chemical composition of each sample was done by XRF analysis using the S8 Tiger Bruker, X-ray Fluorescence Spectrometer and analysed on Spectra Plus software. Pre-testing preparation was carried out on samples, and each ran three times per observation during test. X-ray diffraction was carried out on samples with a Bruker D8 advance automation software-controlled diffractometer using Cu Kα radiation. The XRD traces were measured from 8° to 90° 2θ at a 0.02° 2θ step size. Fig. 3 shows the diffraction pattern as well as the mineral composition for the ashes and the copper slag in comparison. From the figure, copper slag is amorphous, while the fly ash exhibits some crystalline peaks of mainly quartz, mullite, anhydrite, and lime. This is consistent with the data obtained from the XRF analysis of the ash samples which showed a higher CaO percentage in M_B.

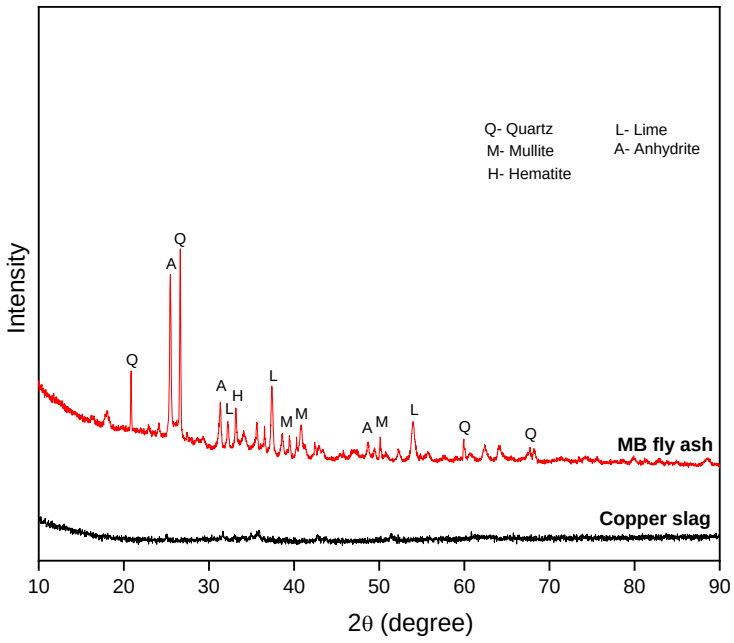

Figure 3: Qualitative XRD of fly ashes and copper slag

2.2.2. Geopolymer Paste Preparation

A mix design was prepared for fly ash and milled copper slag combination in 100:0, 50:50, 60:40, 70:30, and 80:20 blend ratio, respectively. The two material blends were mixed thoroughly in a Hobart mixer for 3 mins before the sodium carbonate powder content was added to the source material. The addition of soda ash in powder to the mix was to efficiently use the initial heat release from the alkaline in the mix to aid the process [23]. Mixing of the alkaline activator and precursors continued for 2 mins at 200rpm till homogeneity was achieved in the mix. Thereafter water was added slowly to the mix and combined thoroughly in the mixer for 3 mins until consistency was achieved. A liquid to solid ratio of 0.3 was maintained for all mix designs except for samples made from 100% FA content which required more water content to achieve the same flow consistency of the other attained mixes. Mix design for the experiment is as detailed in Table 2.

Paste mixture was cast in 50x50x50 mm steel moulds for all derived mix types. The specimens prepared were labelled based on a nomenclature derived from mix content. For example, $50MB50C_SSA_1$ is a specimen made from 50% FA, 50% C_S and 0.32 ratio of soda ash to source material composition. While a specimen with SA_2 will denote 0.40 soda ash

composition ratio. To explore the influence of curing temperature, cast samples were divided into two groups for heat and ambient curing methods. Heat curing was observed in an electric oven at 80 °C. Demoulding for both ambient cured and heat cured samples was done after 24 hrs. The temperature was maintained on the heat-cured sample for 72 hrs and thereafter removed from the oven. Subsequently, hardened pastes were tested for each variation at the required test dates.

Table 2 Experimental mix design details

Mix ID	Fly ash (g)	Copper Slag (g)	Soda ash	Water/solid ratio (L/S)
$50MB50C_SSA_1$	825	825	0.32	0.3
$50MB50C_SSA_2$	825	825	0.4	0.3
$60MB40C_SSA_1$	990	660	0.32	0.3
$60MB40C_SSA_2$	990	660	0.4	0.3
$70MB30C_SSA_1$	1155	495	0.32	0.3
$70MB30C_SSA_2$	1155	495	0.4	0.3
$80MB20C_SSA_1$	1320	330	0.32	0.3
$80MB20C_SSA_2$	1320	330	0.4	0.3
$100MB0C_SSA_1$	1650	0	0.32	0.438*
$100MB0C_SSA_2$	1650	0	0.4	0.438*

*water requirement for samples with solely fly ash content

2.2.3. Testing

2.2.3.1. Compressive strength test

Mechanical property considered in this study is mainly compressive strength. The measurement was done on a servohydraulic testing machine with a load capacity of 600 kN on the hardened geopolymer pastes. The rate of loading was set at 0.9 kN/s until failure for all tested samples. Three test cubes from each specimen were used in the strength evaluation at 3, 7, and 28 days in accordance with ASTM C109. Fragments from each specimen were collected for further analysis. Table 3 gives the details for each specimen as well as recorded compressive strength.

3. Results and Discussion

3.1. Cube Sample Qualitative Observation

Hardened paste samples exhibited initial mild efflorescence formation for samples cured at ambient condition and temperature lower than 65 °C. However, efflorescence on samples were lower a than those associated with NaOH activation [25]. This tendency for efflorescence formation is due to the presence of excess alkali [2]. However, at latter ages of samples after 28 days this effect is less prominent, which may be in relations to moisture loss within the matrix. Shrinkage and crack development is also observed for samples cured at ambient condition. 60FA40CSSA1 and 50MB50CSSA1 samples showed the least efflorescence including absence in some cases. Copper slag dark coloration and constituent percentage in precursor blend tends to be a contributing factor to least efflorescence appearance in samples with high copper slag composition.

Figure 4: Cube sample efflorescence

3.2. Cube Sample Characterisation

XRF analysis of paste samples with different blend ratio is shown in Table 3. From the table, major oxide concentrations are SiO_2, Na_2O, Fe_2O_3, Al_2O_3, and CaO in that order. Evidently, the Iron oxide content of resulting product increased in all FA-CS blends from the introduction of copper slag to the mix. The same observation applies to sodium oxide concentration which increased up to 21.90% after soda ash activation in comparison with less than 1% precursor oxide composition presented in table 1. SiO_2 concentration in hardened pastes of different blends were proportional with fly ash volume. Notably, SO_3 concentration decreased significantly in 60:40 fly ash-copper slag sample mix, and nearly 50% of those recorded for 100:0 whole fly ash mix. This is a result of high SO_3 concentration in the fly ash type utilized. Therefore, copper slag replacement enhanced the reduction of the sulphide in the activated material. The significance of these major oxide concentration is discussed in relation of blend ratio to compressive strength of hardened FA-CS paste.

Table 3 Mix sample percentage oxide composition

Material	SiO_2	Al_2O_3	CaO	Fe_2O_3	SO_3	MnO	Na_2O	MgO
$50M_B50C_SSA_1$	23.60	15.70	13.70	19.00	4.60	0.15	20.00	1.18
$60M_B40C_SSA_1$	22.70	14.50	11.80	21.90	3.90	0.13	21.90	1.20
$70M_B30C_SSA_1$	23.00	15.30	12.40	20.80	4.20	0.14	20.50	1.18
$80M_B20C_SSA_1$	25.10	16.60	15.10	15.20	5.22	0.17	19.60	1.14
100 $M_B0C_SSA_1$	27.00	19.40	19.50	6.43	6.06	0.22	18.20	1.18

3.3. Influence of Blend Ratio on Compressive Strength

The average cube samples compressive strength measured for five different compositions at 3, and 7 days are presented in Figure 4. As shown in the figure, the observed strength trend with age confirms similar results on strength development in alkaline activated systems from previous studies[19] with the exception of $80M_B20C_SSA_1$ with negligible increase. For all FA:CS blend ratio studied, 60:40 blend mix exhibited the highest early strength across the aging. This implies it has the best binding property or gel formation. At high fly ash volume, depolymerization within the material occurs slowly, which may be attributed to non-participation of bulk material in the reaction[15]. Consequently, resulting in lower compressive strength as well as virtually nonsignificant change with other variables. The chemical composition of the precursors and activated product in this study is used to further elucidate the influence of blend ratio with links to compressive strength. Contributory role of copper slag in the blend is explained with the Fe_2O_3 content of product as shown in table 3. The 60:40 blend mix with the optimum compressive strength had the highest compositional percentage of iron oxide which increased with sample compressive strength among the different blends. This observation supports earlier observation by [13], [26] on the impact of iron in the strength development of activated material. Fe_2O_3 acts as a foreign nucleation during reaction as well as a nano filler to the matrix pore structure[26]. Although some studies[1] have attributed increase in compressive strengths to high contents of CaO, the observation in this study however differs. The mix with the highest CaO concentration developed lower strength and vice versa.

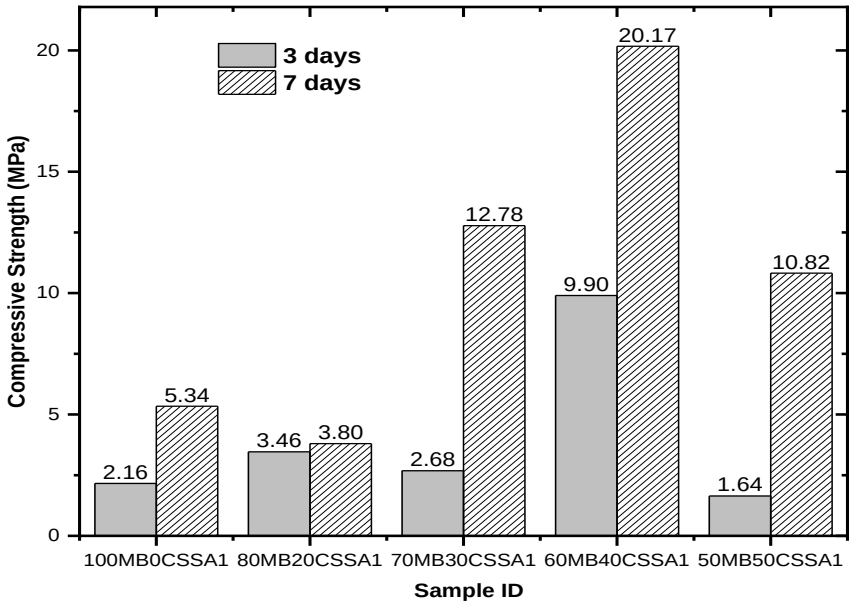

Figure 4: Compressive strength of sample mix

Compressive strength of hardened pastes increased with copper slag addition and peaks at 40 percent slag replacement of fly ash before strength decrease at 50% copper slag composition for the studied blends. Optimum combination of fly ash and copper slag at 60 and 40% respectively resulted in better compressive strength. At high fly ash volume however, paste strength is lowest despite the high CaO, Al_2O_3, and SiO_2 ash composition. Possible minima composition for better performance exists between 40 and 50% copper slag content. Therefore, the optimum composition for this slag type usage in alkaline activation with soda ash is about 40 percent of precursor.

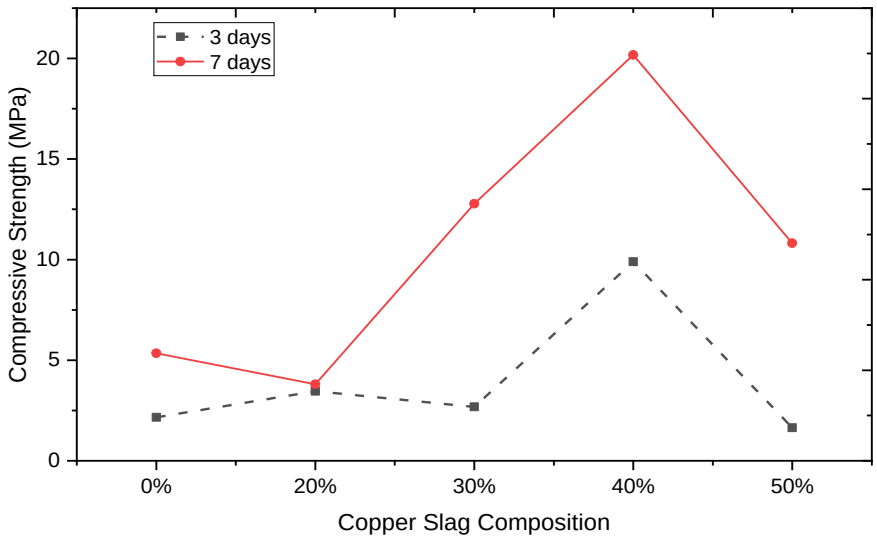

Figure 5: Influence of copper slag addition in sample mix

3.5. Influence of Soda Ash Concentration on Compressive Strength

The effect of soda ash concentration in the mix is illustrated in Figure 6 using two mixes, $60M_B40C_S$ and $100M_B0C_S$ with the highest and lowest boundary compressive strength respectively. As seen with both mixes, increase in activator dosage from 0.32 (A1) to 0.40 (A2) results in higher strength in the hardened paste. Increase in pH of the system from higher activator dosage encouraged the rate of Al and Si dissolution, therefore enhancing more gel formation[27]. At 0.32 soda ash concentration, the strength after 3-day curing was low particularly in sole fly ash mix of $100M_B0C_SA_1$ attaining only 2.16 MPa. Though with an increase in curing time under the same condition, there was considerable improvement in compressive strength to over a 100 percent of 3-day compressive strength. Initial low strength development in this mix suggests insufficient alkali activation and pozzolanic reaction[15]. At a higher dosage of 0.40 however, the strength increase between curing age is not as significant as observed with 0.32 dosage. Also at this dosage, the initial 3-day compressive strength was similar for both $60M_B40C_SSA_2$ and $100M_B0C_SSA_2$ mixes and increased up to a maximum value of 24.38 MPa for $60M_B40C_SSA_2$ sample at 7-day. Overall, the compressive strength of FA/CS activated material increases with increase in Na_2O from soda ash.

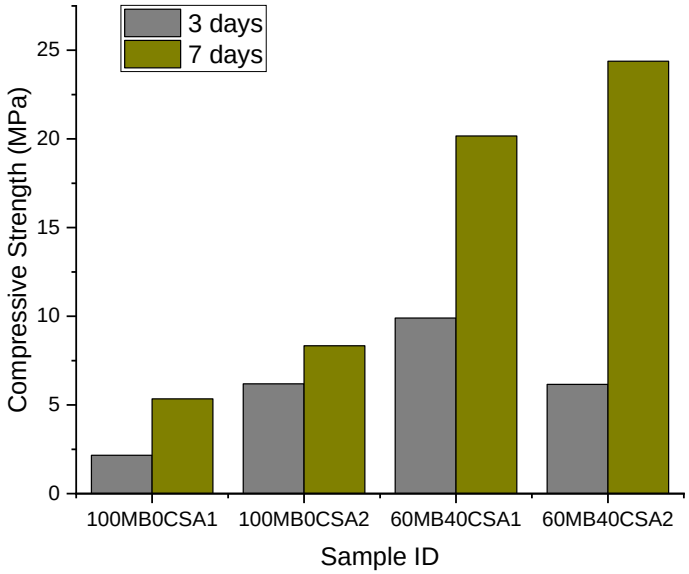

Figure 6: Effect of soda ash composition on compressive strength of paste

3.6. Influence of curing temperature on compressive strength

The evolution of compressive strength for paste mixes over a range of temperature curing is shown in fig. 7. All mixes showed an initial rapid increase in strength value from 45 to 65 °C compared with strength again from 65 to 80°C. Although there is a slight increase as seen in $70M_B30C_SSA_2$ and $80M_B20C_SSA_2$ samples, 7- and 28-day strength was similar in most. At 7-day, the response of the sample to temperature increase was most significant in $50M_B50C_SSA_2$, the least in $80M_B20C_SSA_2$, while a higher temperature of 80 °C is ideal for strength development in the earlier optimised mix of 60:40 fly ash/slag mix. Early age strength at 45 °C for all samples was below 4 MPa. This suggests a temperature of 45 °C and below seems unsuitable with this type of activation system. Alkali activation of the FA/CS mixes is accelerated by heat curing, resulting in higher compressive strength as the material age. This agrees with [27] on the behaviour of heat-cured alkali-activated CS concrete. For this study, 65 and 80 °C are thus temperature conditions of interest around where a trade-off between energy savings and compressive strength gain could be established.

Figure 7. Compressive strength of pastes at different curing temperatures: (a) 7-day; (b) 28-day

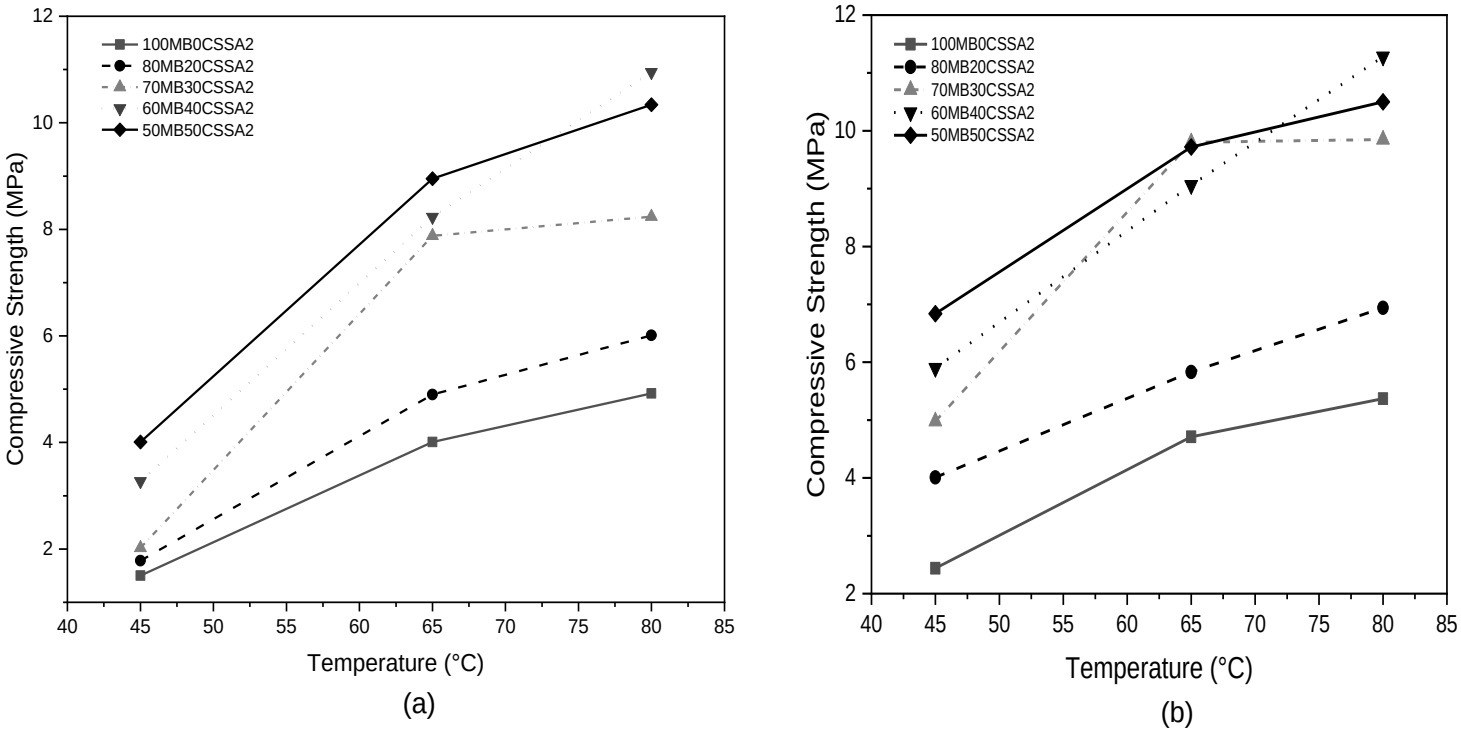

4. Conclusion

Compressive strength development in fly ash-copper slag-activated systems using a mild alkaline activator was investigated in this study. The influence of factors such as blend ratio, activator concentration, and the curing temperature was considered. The conclusions are as follows:

1. Activator concentration of soda ash and the blend ratio of precursors were the most significant influencing factor on both early and later age compressive strength development in fly ash-copper slag activated material. 0.40 soda ash to precursor ratio sufficiently raised the pH of the matrix enough to enhance the dissolution requirement of Al and Si species. optimum compressive strength of 24.66 MPa was obtained at 28 days for 60:40 fly ash/copper slag blend ratio at a curing temperature of 80 degrees.
2. The curing temperature effect largely influences the early strength gain in the material. When early strength is desired, heat curing at 80 °C temperature was very effective for all mix types in this study. Though the effect is less significant at the latter age of the sample after 7- day. The reduction in fly-ash content with an increase in copper slag content results in a consistent increase in strength for curing temperatures of 45 and 65 degrees.
3. High fly ash volume blends performed the least under all factors considered using soda ash activator. However, with the addition of copper slag in a tailored mix design, compressive strength is improved.

Acknowledgment

The authors would like to acknowledge the financial support of the Office of Research, Development, and Innovation (ORDI) of the Botswana International University of Science and Technology under grant S00177 in the actualization of this publication.

References

[1] A. Leonard Wijaya, J. Jaya Ekaputri, and Triwulan, "Factors influencing strength and setting time of fly ash based-geopolymer paste," *MATEC Web Conf.*, vol. 138, 2017.

[2] Z. Zhang, J. L. Provis, A. Reid, and H. Wang, "Fly ash-based geopolymers: The relationship between composition, pore structure and efflorescence," *Cem. Concr. Res.*, vol. 64, pp. 30–41, 2014.

[3] G. Kovalchuk, A. Fernández-Jiménez, and A. Palomo, "Alkali-activated fly ash: Effect of thermal curing conditions on mechanical and microstructural development - Part II," *Fuel*. 2007.

[4] M. Criado, A. Fernández-Jiménez, and A. Palomo, "Alkali activation of fly ash. Part III: Effect of curing conditions on reaction and its graphical description," *Fuel*, 2010.

[5] X. Ke, S. A. Bernal, and J. L. Provis, "Controlling the reaction kinetics of sodium carbonate-activated slag cements using calcined layered double hydroxides," *Cem. Concr. Res.*, vol. 81, pp. 24–37, 2016.

[6] A. A. Aliabdo, A. E. M. Abd Elmoaty, and M. A. Emam, "Factors affecting the mechanical properties of alkali activated ground granulated blast furnace slag concrete," *Constr. Build. Mater.*, vol. 197, pp. 339–355, 2019.

[7] S. A. Bernal, R. S. Nicolas, J. S. J. van Deventer, and J. L. Provis, "Alkali-activated slag cements produced with a blended sodium carbonate/sodium silicate activator," *Adv. Cem. Res.*, vol. 28, no. 4, pp. 262–273, 2015.

[8] C. Panagiotopoulou, E. Kontori, T. Perraki, and G. Kakali, "Dissolution of aluminosilicate minerals and by-products in alkaline media," *J. Mater. Sci.*, vol. 42, no. 9, pp. 2967–2973, 2007.

[9] S. K. Nath, S. Maitra, S. Mukherjee, and S. Kumar, "Microstructural and morphological evolution of fly ash based geopolymers," *Constr. Build. Mater.*, vol. 111, pp. 758–765, 2016.

[10] I. Garcia-Lodeiro, A. Palomo, and A. Fernández-Jiménez, *Crucial insights on the mix design of alkali-activated cement-based binders*. Woodhead Publishing Limited, 2014.

[11] I. Garcia-Lodeiro, A. Palomo, and A. Fernández-Jiménez, "A review of alkaline activation: new analytical perspectives," *Handb. Alkali-Activated Cem. Mortars Concr.*, no. April 2016, pp. 19–47, 2015.

[12] Z. Yan, Z. Sun, J. Yang, H. Yang, Y. Ji, and K. Hu, "Mechanical performance and reaction mechanism of copper slag activated with sodium silicate or sodium hydroxide," *Constr. Build. Mater.*, vol. 266, p. 120900, 2021.

[13] P. N. Lemougna, K. J. D. MacKenzie, G. N. L. Jameson, H. Rahier, and U. F. Chinje Melo, "The role of iron in the formation of inorganic polymers (geopolymers) from volcanic ash: A 57Fe Mössbauer spectroscopy study," *J. Mater. Sci.*, vol. 48, no. 15, pp. 5280–5286, 2013.

[14] S. Onisei, K. Lesage, B. Blanpain, and Y. Pontikes, "Early Age Microstructural Transformations of an Inorganic Polymer Made of Fayalite Slag," *J. Am. Ceram. Soc.*, vol. 98, no. 7, pp. 2269–2277, 2015.

[15] T. Zhang, H. Jin, L. Guo, W. Li, J. Han, A. Pan, and D. Zhang, "Mechanism of Alkali-Activated Copper-Nickel Slag Material," *Adv. Civ. Eng.*, vol. 2020, 2020.

[16] A. A. Mohammed, H. U. Ahmed, and A. Mosavi, "Survey of mechanical properties of geopolymer concrete: A comprehensive review and data analysis," *Materials (Basel).*, vol. 14, no. 16, 2021.

[17] P. De Silva, K. Sagoe-Crenstil, and V. Sirivivatnanon, "Kinetics of geopolymerization: Role of Al2O3 and SiO2," *Cem. Concr. Res.*, vol. 37, no. 4, pp. 512–518, 2007.

[18] P. Zhang, Z. Gao, J. Wang, J. Guo, S. Hu, and Y. Ling, "Properties of fresh and hardened fly ash/slag based geopolymer concrete: A review," *J. Clean. Prod.*, vol. 270, p. 122389, 2020.

[19] S. Ukritnukun, P. Koshy, A. Rawal, A. Castel, and C. C. Sorrell, "Predictive model of setting times and compressive strengths for low-alkali, ambient-cured, fly ash/slag-based geopolymers," *Minerals*, vol. 10, no. 10, pp. 1–21, 2020.

[20] S. Puligilla and P. Mondal, "Role of slag in microstructural development and hardening of fly ash-slag geopolymer," *Cem. Concr. Res.*, vol. 43, no. 1, pp. 70–80, 2013.

[21] J. L. Provis, A. Palomo, and C. Shi, "Advances in understanding alkali-activated materials," *Cement and Concrete Research*. 2015.

[22] F. Sajedi and H. A. Razak, "Comparison of different methods for activation of ordinary Portland cement-slag mortars," *Constr. Build. Mater.*, vol. 25, no. 1, pp. 30–38, 2011.

[23] T. Suwan and M. Fan, "Effect of manufacturing process on the mechanisms and mechanical properties of fly ash-based geopolymer in ambient curing temperature," *Mater. Manuf. Process.*, vol. 32, no. 5, pp. 461–467, 2017.

[24] P. Risdanareni, P. Puspitasari, and E. Januarti Jaya, “Chemical and Physical Characterization of Fly Ash as Geopolymer Material,” *MATEC Web Conf.*, vol. 97, 2017.
[25] G. Ishwarya, B. Singh, S. Deshwal, and S. K. Bhattacharyya, “Effect of sodium carbonate/sodium silicate activator on the rheology, geopolymerization and strength of fly ash/slag geopolymer pastes,” *Cem. Concr. Compos.*, vol. 97, pp. 226–238, 2019.
[26] E. A. Obonyo, E. Kamseu, P. N. Lemougna, A. B. Tchamba, U. C. Melo, and C. Leonelli, “A sustainable approach for the geopolymerization of natural iron-rich aluminosilicate materials,” *Sustain.*, vol. 6, no. 9, pp. 5535–5553, 2014.
[27] J. Singh and S. P. Singh, “Utilization of alkali-activated copper slag as binder in concrete,” *Front. Struct. Civ. Eng.*, vol. 15, no. 3, pp. 773–780, 2021.